

# Verified Bit and Power Allocation for MIMO Systems: A Comparison of SVD Based Techniques With GMD

Ekaterina Auer<sup>ab</sup> and Andreas Ahrens<sup>ac</sup>

## Abstract

Methods with result verification have been applied in different practical contexts, for example, in such diverse areas as robotics, computer graphics, or chemistry. Such methods help to verify the result of a computer simulation, additionally taking into account possibly present bounded uncertainty in a deterministic way. Modeling and simulation of multiple-input multiple-output (MIMO) systems has not received much attention from this angle. Nowadays, increasing the capacity of communication links by using the MIMO mechanism is an essential part of various wireless communication standards.

In this paper, we consider the channel separation stage in the overall modeling and simulation process for MIMO systems and compare the singular value decomposition (SVD) and the geometric mean decomposition (GMD) based approaches from the point of view of the achievable bit error ratio (BER) under good and poor scattering conditions. As a special focus, we use interval methods to verify the result and to deal with the appearing epistemic uncertainty. Additionally, we consider resource allocation in detail, which mostly makes sense only for the SVD approach since the goal of the GMD based one is to avoid it. However, this has been studied only asymptotically until now and needs confirmation. We propose a combined analytical-numerical approach to simulate resource allocation relying on verified techniques. The theoretical results are illustrated and the comparison is performed using simulated data for an uncorrelated and a correlated MIMO system with four receiving and four transmitting antennas.

**Keywords:** MIMO, methods with result verification, SVD, GMD, resource allocation, Lagrange multipliers

---

<sup>a</sup>University of Applied Sciences Wismar, Germany

<sup>b</sup>E-mail: [ekaterina.auer@hs-wismar.de](mailto:ekaterina.auer@hs-wismar.de), ORCID: [0000-0003-4059-3982](https://orcid.org/0000-0003-4059-3982)

<sup>c</sup>E-mail: [andreas.ahrens@hs-wismar.de](mailto:andreas.ahrens@hs-wismar.de), ORCID: [0000-0002-7664-9450](https://orcid.org/0000-0002-7664-9450)

# 1 Introduction

In the last decades, the multiple-input multiple-output (MIMO) method for transmitting information has become an essential mechanism in wireless communications. This strategy of placing multiple antennas both at the transmitter and receiver sides can be shown to improve the capacity and the integrity of wireless systems [4, 7, 21]. In this paper, we work with simulated systems relying on a simple linear stochastic model for a frequency flat<sup>1</sup> MIMO link consisting of  $n_T$  transmitting and  $n_R$  receiving antennas given as

$$\vec{y} = H \cdot \vec{a} + \vec{n}, \quad \vec{y}, \vec{n} \in \mathbb{C}^{n_R}, \quad \vec{a} \in \mathbb{C}^{n_T}, \quad H \in \mathbb{C}^{n_R \times n_T} . \quad (1)$$

Here,  $\vec{y}$  is the received data vector,  $\vec{a}$  is the transmitted signal vector,  $\vec{n}$  is the vector of the additive white Gaussian noise at the receiver side with the zero mean and the standard deviation  $\sigma$  in both real and imaginary parts. The investigated (frequency flat) channel profile generates interferences between the different antenna's data streams but no intersymbol interference is present at the receiver input. We assume that the standard deviation of the noise is computed as

$$\sigma = \sqrt{\frac{P_s}{2 \cdot 10^{\frac{E_s}{N_0}/10}}} .$$

In this formula,  $P_s$  is the available transmit power and  $\frac{E_s}{N_0}$  in dB is the signal-to-noise ratio (SNR), where  $E_s$  denotes the symbol energy and  $N_0$  the noise power spectral density. Additionally, we assume that the throughput of the MIMO system is fixed at a certain desired value.

The channel matrix  $H$  from Eq. (1) describes each individual path from every transmitting antenna to every receiving antenna. In order to simulate the actual paths, the Rayleigh distribution is used in wireless communications. That is, the coefficients of the  $(n_R \times n_T)$  matrix  $H$  are simulated as independently and identically distributed Rayleigh fading channels [20] with the equal standard deviation  $\delta$ .

In Figure 1, the general modeling and simulation process for a MIMO system is shown. The first step is to define the structure of the MIMO system. The spatial placement of the antennas is responsible for scattering conditions being good or poor, or, in other words, for creating an uncorrelated (good conditions) or correlated system. In the next step, the channel matrix of the link needs to be identified, which can be done, for example, via least squares optimization using pilot sequences [23]. In this paper, we rely on simulated matrices obtained by the Rayleigh distribution as described, for example, in [1]. The last two steps in the process are in the focus of the present study: interference suppression (channel separation) and resource allocation with the goal of optimizing the quality criterion of the bit error ratio (BER). Additionally, we consider the influence of the scattering conditions.

---

<sup>1</sup>i.e., a single filter channel tap is enough to represent it; the channel can be described by a single matrix  $H$  [22]

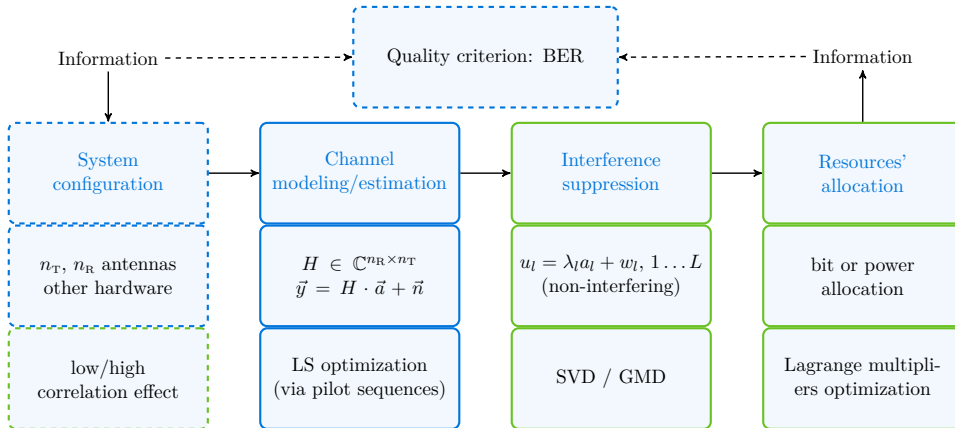


Figure 1: General stages in the MIMO modeling and simulation process. The stages this paper focuses on are shown in green.

The intention behind the interference suppression is to create  $n = \min \{n_R, n_T\}$  separate single-input single-output (SISO) communication channels (ideally, without interference) corresponding to the original MIMO channel  $H$  using the appropriate precoding and postcoding techniques [9, 18]. The usual approach here is to employ the singular value decomposition (SVD) of the matrix  $H$  creating SISO channels of unequal weights, which, therefore, have different performance wrt. the BER. However, it is also possible to use the geometric mean decomposition (GMD) technique producing  $n$  *identical* separate channels at the cost of remaining interferences which can be, however, removed from the system by using interference cancellation schemes [10].

Whereas it is advantageous to optimize allocation of resources in the last step of the process in case of the SVD [18], the GMD based approach is reported to be optimal for high SNR, that is, low  $\sigma$ , meaning that resources such as bits per symbol and power can be distributed uniformly among the (active) SISO channels [10]. To our best knowledge, there is no systematic comparison between the SVD and GMD based approaches wrt. the best achievable BER, which additionally considers the difference between correlated and uncorrelated systems. Our intention in this paper is to close the gap with a further focus on verifying the obtained results and quantifying bounded uncertainty via an additional deterministic approach, namely, interval analysis [15].

Interval analysis and other methods with *result verification* can describe and forward-propagate<sup>2</sup> bounded uncertainty in parameters deterministically if an appropriate implementation of a mathematical model is possible. This *computerized model* can be symbolic (mathematical equations describing the system of interest)

<sup>2</sup>Although approaches for inverse propagation exist (a good overview is in [19]), the more usual application is for the forward problem

or algorithmic (code). There are many ready-made implementations of interval counterparts to the usual floating point based software: set arithmetic [5, 13] (basic operations  $+$ ,  $-$ ,  $\cdot$ ,  $/$ ; elementary functions such as the sine) and more complex methods such as those for solving linear and non-linear systems of equations or initial value problems [8, 16]. Many more references can be provided in each case. Originally, methods with result verification were developed to address the question of reliability by proving formally that the outcome of a simulation implemented on a computer was correct (assuming that the underlying implementation was correct). The results are usually sets of floating point numbers which with certainty contain the exact solution to the computerized model. The advantage is that usual numerical assumptions such as truncation or discretization cannot lead to a wrong solution and their negative influence does not remain undetected if result verification is used. A common drawback is the possibility of too conservative bounds for the solution sets (e.g., between  $-\infty$  and  $+\infty$ ) caused by the dependency problem or the wrapping effect [14]. Aside from previous work by the authors, interval analysis has been applied to MIMO systems in [24], however, in the context of identification.

The structure of the paper is as follows: In Section 2, the mathematical background of the SVD and GMD decomposition is briefly outlined along with the formulas for the corresponding BER (including quantification of possible bounded epistemic uncertainty). In Section 3, the process of resource allocation is considered from the mathematical point of view. In Section 4, we apply the suggestions from Section 3 to a benchmark MIMO system with four receiving and four transmitting antennas for which a correlated and uncorrelated situations are simulated. We consider bit and power allocation for this system and compare the SVD and GMD channel separation, especially detailed for two active layers. Conclusions are in the last section.

## 2 Interference Suppression: SVD, GMD, BER

The channel matrix  $H$  identified at the second stage in the MIMO modeling and simulation process from Figure 1 is usually dense so that it is not possible to distinguish separate SISO layers. In this section, we give a brief outline of common techniques to determine the non-interfering SISO layers corresponding to the channel described by  $H$  using the singular value and the geometric mean decompositions in Subsections 2.1 and 2.2, respectively. The description in Subsection 2.1 relies on [18], in Subsection 2.2 on [11]. Note that the SVD based technique is at the moment the standard one. Moreover, the interference suppression between the SISO channels described here is ideal and works in theory. In practice, there can still be residual interference. In Subsection 2.3, we provide the formulas for the corresponding BER along with its upper bound for the case that certain parameters are not known exactly.

## 2.1 SVD Based Channel Separation

The channel matrix from Eq. (1) is decomposed as  $H = U \cdot \Sigma \cdot V^\dagger$ , where  $U$  and  $V$  are unitary matrices,  $\Sigma$  is the diagonal matrix with real elements and  $V^\dagger$  denotes the Hermitian transpose of  $V$ . The matrix  $\Sigma$  contains the positive square roots of the eigenvalues  $\xi_l$  of  $H^\dagger H$  in descending order on the main diagonal (*singular values* denoted by  $\lambda_l = \sqrt{\xi_l}$  throughout the paper). If a pre-processed data vector  $\vec{x} := V \cdot \vec{a}$  is considered and the corresponding receive signal  $\vec{z} := H\vec{x} + \vec{n}$  is post-processed by  $U^\dagger$ , then the new receive signal is

$$\vec{u} := U^\dagger \vec{z} = U^\dagger (U \Sigma V^\dagger) V \vec{a} + U^\dagger \vec{n} = \Sigma \vec{a} + \vec{w} \quad , \quad (2)$$

where the vector  $\vec{a}$  is the transmitted signal vector and  $\vec{n}$  is the Gaussian noise vector as explained in the Introduction. In this way, the MIMO link is transformed (ideally) into  $n = \min\{n_T, n_R\}$  independent, non-interfering SISO layers  $u_l$  having (unequal) weights  $\lambda_l$  (satisfying the condition  $\lambda_1 > \lambda_2 > \dots > \lambda_n$ ):

$$u_l = \lambda_l a_l + w_l \quad \text{for } l = 1 \dots n \quad . \quad (3)$$

Out of those, only  $L = 2, \dots, n$  layers need to be actively used while transmitting information. Since the weights for each layer are different, it is profitable to optimize the allocation of such resources as transmit power. In poor scattering conditions with high antenna correlation, where the weighting of the SISO channels might turn strongly unequal, such optimization gains in importance but is challenging. A unique indicator of the unequal weighting of the MIMO layers is the ratio  $\vartheta$  between the smallest and the largest singular value which characterizes the correlation effect (and is also the condition number of the matrix  $H$ ).

## 2.2 GMD Based Channel Separation

The channel matrix from Eq. (1) is decomposed as  $H = Q \cdot R \cdot P^\dagger$ , where  $P$  and  $Q$  are semiunitary<sup>3</sup> matrices,  $R \in \mathbb{R}^{n \times n}$  is an upper triangular matrix with identical diagonal elements. After precoding the signal  $\vec{a}$  by  $P$  at the transmitter side ( $\vec{x} = P\vec{a}$ ) and postcoding  $\vec{z} = H\vec{x} + \vec{n}$  by  $Q^\dagger$  at the receiver side, the model in Eq. (1) turns into

$$\vec{u} = R\vec{a} + Q^\dagger \vec{n} = R\vec{a} + \vec{v} \quad . \quad (4)$$

By using appropriate nulling and cancellation approaches [9], it is possible to obtain  $n$  parallel, non-interfering SISO links of the form

$$u_l = \lambda \cdot a_l + v_l \quad \text{with equal weights } \lambda = \left( \prod_{l=1}^n \lambda_l \right)^{\frac{1}{n}} \quad . \quad (5)$$

Since all SISO layers are equal, it should not be necessary to optimize wrt. the amount of bits per symbol or power, which can be chosen to be the same for each

<sup>3</sup>that is, non-square matrices either the rows or columns of which are orthonormal

active layer [10]. However, as will be described in Subsection 2.3, it might still be advantageous to select the number of active layers (i.e., the number of activated MIMO layers  $L = 2, \dots, n$  for the data transmission within an  $n_T \times n_R$  MIMO system) to be less than  $n$ . The actual value of  $\lambda$  strongly depends on  $L$  and can be

computed as  $\lambda = \left( \prod_{l=1}^L \lambda_l \right)^{\frac{1}{L}}$ .

Note that we do not consider explicitly the added uncertainty appearing due to the use of precoding/postcoding (SVD) or nulling/cancellation (GMD) in this paper. This point has been addressed, for example, in [3].

### 2.3 BER for SVD and GMD Separated Channels

For simple MIMO transmission channel and data source models, the BER can be computed analytically [3]. In particular, for quadrature amplitude modulated signals, the bit error probability for a transmission SISO layer  $l$  is given as

$$p_b^{(l)} = \frac{2}{m_l} \left( 1 - 2^{-\frac{m_l}{2}} \right) \cdot \operatorname{erfc} \left( \frac{\lambda_l \sqrt{3 \cdot P_s^{(l)}}}{2\sigma \sqrt{2^{m_l} - 1}} \right) \quad (6)$$

if the SVD is used. It depends on the amount of bits per symbol  $m_l$  (and the constellation size  $M_l = 2^{m_l}$ ), the noise standard deviation  $\sigma$ , the available transmission power per layer  $P_s^{(l)}$  and the singular value  $\lambda_l$  corresponding to the considered layer;  $\operatorname{erfc}(\cdot)$  is the complementary error function. The desired throughput is denoted by

$$T = \sum_{l=1}^L \log_2 M_l = \sum_{l=1}^L m_l \quad (7)$$

and considered to be constant throughout the paper. The BER for the whole MIMO link is the sum of probabilities per layer modified with the respective number of bits per layer and the throughput:

$$p_b = \frac{1}{T} \sum_{l=1}^L m_l \cdot p_b^{(l)} = \frac{2}{T} \sum_{l=1}^L \left( 1 - 2^{-\frac{m_l}{2}} \right) \cdot \operatorname{erfc} \left( \frac{\lambda_l \sqrt{3 \cdot P_s^{(l)}}}{2\sigma \sqrt{2^{m_l} - 1}} \right) \quad (8)$$

The weights  $\lambda_l$  are not necessarily equal for each SISO layer if the SVD is used, which is usually countered by assigning power to layers in the optimal way instead of uniformly ( $P_s^{(l)} = \frac{P_s}{L} \rightarrow P_s^{(l)} = \pi_l^2 \cdot \frac{P_s}{L}$ ). That is, employing the analytical BER representation as a cost function, a MIMO system can be optimized wrt. the parameters  $\pi_l$ , for example, with the help of the Lagrange multipliers approach. The noise variance  $\sigma^2$  is usually considered to be fixed, but it is possible to optimize the BER still further with the help of bit allocation. Here, the number of bits per symbol  $m_l$  for  $L$  active layers is computed such that the BER is minimized. Since  $m_l$  are natural numbers, the integer optimization problem needs to be solved.

The BER of a correlated system can become significantly higher than that of an uncorrelated one.

Another possibility to deal with the unequal weights and to minimize the BER is to use GMD as described in Subsection 2.2. The formula in Eq. (8) remains almost the same except that, instead of the singular values  $\lambda_l$  of the channel matrix  $H$ , their geometric mean  $\lambda$  is used for each active layer to compute  $p_b^{(l)}$ . Additionally, if the number of bits per symbol is chosen to be the same ( $m = m_1 = m_2 = \dots = m_L$ ) and the overall power  $P_s$  is equally distributed among the  $L$  active layers, the BER in Eq. (8) simplifies to

$$p_{b,\text{GMD}} = \frac{mL}{T} p_b^{(*)} = \frac{2L}{T} \left(1 - 2^{-\frac{m}{2}}\right) \cdot \operatorname{erfc} \left( \frac{\lambda}{2\sigma} \sqrt{\frac{3 \cdot P_s}{L(2^m - 1)}} \right). \quad (9)$$

Note that if  $T$  is constant,  $m = \frac{T}{L}$ . Since  $m \in \mathbb{N}$ , the number of active layers  $L$  should be chosen such that  $\frac{T}{L} \in \mathbb{N}$ .

Since the BER in both (8) and (9) is essentially a sum of positive values of the corresponding  $p_b^{(l)}$ , it might be profitable to choose the number of active layers  $L$  to be less than  $n$ , possibly switching off the layer with the highest  $p_b^{(l)}$  in the case of SVD.

If the formula in Eq. (8) (or Eq. (9)) is used to compute the overall BER, it is obvious that the major characteristics influencing this quality criterion are the singular values  $\lambda_l$  (layer weights), the standard deviation of the noise  $\sigma$ , the numbers of bits per symbol  $m_l$ , the transmit power per layer  $P_s^{(l)}$  and the number of activated layers  $L$ . As already mentioned, the throughput  $T$  is assumed to be constant. Initially,  $P_s^{(l)} = P_s/L$  is equal for each layer and is optimized during the stage of power allocation. Optimizing wrt.  $m_l$  is the purpose of bit allocation. Choosing the number of active layers  $L$  also belongs to the stage of resource allocation. If it holds for the remaining parameters that  $\lambda_l \in [\underline{\lambda}_l, \bar{\lambda}_l]$ , where  $\underline{\lambda}_l, \bar{\lambda}_l$  are known lower and upper bounds, respectively, and the standard deviation  $\sigma \in [\underline{\sigma}, \bar{\sigma}]$ , then a conservative upper bound on the BER can be obtained using the rules of interval arithmetic as

$$p_b(\sigma, \lambda_1 \dots \lambda_L) \leq \frac{2}{T} \sum_{l=1}^L \left(1 - 2^{-\frac{m_l}{2}}\right) \cdot \operatorname{erfc} \left( \frac{\underline{\lambda}_l}{2\bar{\sigma}} \sqrt{\frac{3 \cdot P_s^{(l)}}{2^{m_l} - 1}} \right) \quad (10)$$

(cf. [2]). That is, due to monotonicity of the involved functions, it is not necessary to work with actual ranges but with their bounds only, which makes verified optimization easier. Note that the upper bound for  $\sigma$  would be achieved, theoretically, at the SNR below 1dB, which is of no practical interest since the signal would be too ‘noisy’ to be considered useful. Therefore, it is common practice to choose a certain fixed SNR  $\frac{E_s}{N_0}$  in dB (e.g., between 5dB and 20dB) at which the behavior of the MIMO system is studied.

### 3 Bit and Power Allocation

If the SISO channels are separated via the SVD, the overall system can be optimized wrt. the quality criterion of the BER by appropriate allocation of resources. The first factor to consider is the number of active layers  $L$  to use. Next, the amount of information that should be put through each of the active layers  $l = 1 \dots L$  can be optimized (bit allocation). Finally, the power assigned to each active layer can be optimized (power allocation). In this section, we consider these processes in detail. Where necessary, we mention the behavior of the GMD separated MIMO system in the context.

#### 3.1 Bit Allocation

##### 3.1.1 Bit Allocation with Non-Linear Mixed-Integer Programming (Exact)

The number of bits per transmitted symbol and layer influences the overall BER as can be seen from Eq. (8). Optimizing with respect to bits per symbol (that is, with power equally distributed among the  $L$  active layers) is not trivial since  $m_l$  should be positive integers fitting the desired throughput  $T$  from Eq. (7), which leads to a non-linear mixed-integer programming problem [12]. For small numbers of active layers  $L$  and constant throughputs  $T$ , the problem can be treated by considering all admissible combinations of  $m_l \in \{1, 2, \dots, T - L + 1\}$  satisfying the constraint in Eq. (7) and choosing the combination with the smallest  $p_b$  [1]. For small  $T$ , it is easy to implement a routine checking the BER produced by all admissible constellations of  $m_l$ . For example, an overall of 21 combinations needs to be tested for  $T = 8$  (bit/s)/Hz and three active layers ( $L = 3$ ). For high numbers of antennas and higher throughput, this simple routine would be too inefficient wrt. computing time. Even increasing the number of active layers by one (to  $L = 4$ ) results in an increase by 14 combinations (i.e., there are 35 combinations to check). Since  $\lambda_1 > \lambda_2 > \dots > \lambda_L$ , that is, the first layer is the strongest (has the smallest BER), the second is the second strongest and so on, it is usually assumed that also  $m_1 \geq m_2 \geq \dots \geq m_L$ , which corresponds to the practical consideration that stronger layers should transmit more information. This assumption reduces the number of combinations from 21 to five for the example with the three active layers.

As is obvious from Eq. (6), the error probability  $p_b^{(l)}$ , considered as a function of  $\lambda_l > 0$ , decreases monotonically and has a positive range. It is not easy to answer the same question for  $p_b^{(l)}$  as a function of  $m_l$ , even over the limited definition domain  $[1, T - L + 1]$ . It can be monotonically increasing or decreasing with  $m_l$  for some values of  $\lambda_l$ , or not be monotonic at all (cf. the example in Figure 2). However, the range is always positive over  $[1, T - L + 1]$ , as can be easily seen from Eq. (6). The behavior wrt. monotonicity is explained by the derivatives wrt. to  $m_l$  and  $\lambda_l$ :



$$\begin{aligned} \frac{\partial p_b^{(l)}}{\partial m_l} = & -\frac{2}{m_l^2} \left(1 - 2^{-\frac{m_l}{2}}\right) \cdot \operatorname{erfc} \left( \frac{\lambda_l}{2\sigma} \sqrt{\frac{3 \cdot P_s^{(l)}}{2^{m_l} - 1}} \right) + \\ & \frac{\ln 2}{m_l} \cdot \left( 2^{-m_l/2} \cdot \operatorname{erfc} \left( \frac{\lambda_l}{2\sigma} \sqrt{\frac{3P_s^{(l)}}{2^{m_l} - 1}} \right) + \right. \end{aligned} \quad (11)$$

$$\begin{aligned} & \left. \frac{\lambda_l}{\sigma} \sqrt{\frac{3P_s^{(l)}}{\pi}} \cdot \frac{2^{m_l/2}}{\sqrt{2^{m_l} - 1} (2^{m_l/2} + 1)} \cdot \exp \left( -\frac{\lambda_l^2}{4\sigma^2} \frac{3P_s^{(l)}}{(2^{m_l} - 1)} \right) \right) \\ \frac{\partial p_b^{(l)}}{\partial \lambda_l} = & -\frac{2}{m_l \sigma} \sqrt{\frac{3P_s^{(l)}}{\pi (2^{m_l} - 1)}} \cdot \left(1 - 2^{-\frac{m_l}{2}}\right) \cdot \exp \left( -\frac{\lambda_l^2}{4\sigma^2} \frac{3P_s^{(l)}}{(2^{m_l} - 1)} \right). \end{aligned} \quad (12)$$

It holds that  $\frac{\partial p_b^{(l)}}{\partial \lambda_l} < 0$  for  $m_l \geq 1$ ,  $\sigma > 0$  (which is the case). No such simple statement can be derived for  $\frac{\partial p_b^{(l)}}{\partial m_l}$  in Eq. (11) since it contains both positive and negative terms depending on the same parameters and variables. Therefore, it is, strictly speaking, not clear that taking  $m_1 \geq m_2 \geq \dots \geq m_L$  would produce the minimal value for the BER in Eq. (8) under the constraint (7). However, if the BER is computed according Eq. (8), where  $p_b^{(l)}$  is multiplied by the corresponding  $m_l$ , the negative term disappears from the derivative  $\frac{\partial p_b}{\partial m_l}$  making it always positive (cf. Eq. (15)). That is, the overall BER is a sum of functions monotonically increasing with  $m_l$ . Since  $\operatorname{erfc}(\lambda_1) < \operatorname{erfc}(\lambda_2) < \dots < \operatorname{erfc}(\lambda_L)$ , taking  $m_1 \geq m_2 \geq \dots \geq m_L$  (and therefore  $M_1 \geq M_2 \geq \dots \geq M_L$ ) seems a good choice, which is also confirmed experimentally in the next Section.

### 3.1.2 Bit Allocation with Lagrange Multipliers (Approximate)

Another approach to bit allocation is to approximately solve the problem by the Lagrange multipliers method. The task is

$$p_b(m_1, \dots, m_L) \xrightarrow{m_1 \dots m_L} \min \quad \text{s.t.} \quad \sum_{l=1}^L m_l = T \quad \text{where} \quad P_s^{(l)} = \frac{P_s}{L}. \quad (13)$$

The cost function to consider is then

$$J(m_1, \dots, m_L, \mu) = p_b(m_1, \dots, m_L) + \mu \cdot \left( -T + \sum_{l=1}^L m_l \right) \quad (14)$$

if we are interested in the number of bits per symbol  $m_l$ . This formulation disregards that the numbers  $m_l$  should be positive integers and would possibly compute

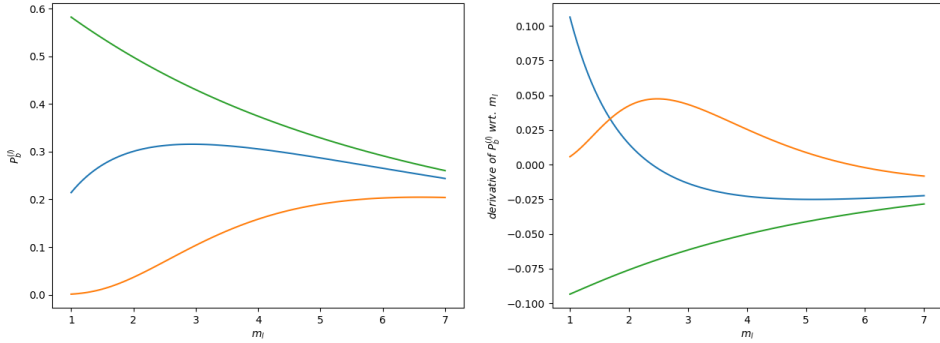


Figure 2: BER  $p_b^{(l)}$  per layer  $l$  with  $P_s^{(l)} = \frac{1}{3}$  as a function of  $m_l$  (left) and its derivative wrt.  $m_l$  (right) for an example system from Subsection 4.1 for  $\lambda_l = 1.3791$  (orange),  $\lambda_l = 0.1609$  (blue) and  $\lambda_l = 0.0013$  (green).

approximate real values for them. The system we need to solve to obtain candidates for the optimal sets of bits per symbol  $m_l$  for  $l = 1 \dots L$  is

$$\frac{\partial J}{\partial m_l} = \frac{\ln 2}{T} \cdot \left( 2^{-m_l/2} \cdot \operatorname{erfc} \left( \frac{\lambda_l \sqrt{3P_s^{(l)}}}{2\sigma \sqrt{2^{m_l} - 1}} \right) + \right. \quad (15)$$

$$\left. \frac{\lambda_l \sqrt{3P_s^{(l)}}}{\sigma \sqrt{\pi}} \cdot \frac{2^{m_l/2}}{\sqrt{2^{m_l} - 1} (2^{m_l/2} + 1)} \cdot \exp \left( -\frac{\lambda_l^2}{4\sigma^2} \frac{3P_s^{(l)}}{(2^{m_l} - 1)} \right) \right) + \mu = 0$$

$$\frac{\partial J}{\partial \mu} = -T + \sum_{l=1}^L m_l = 0 \quad (16)$$

Having computed the enclosures of the approximate real values for  $m_l$ , for example, using a solver for systems of non-linear equations based on methods with result verification (e.g., C-XSC Toolbox [8]), we can choose positive integer values that are the closest to them. Here, rounding to the nearest integer number actually provides the results that fulfil the constraint (cf. Table 1). However, we can also round the first  $L - 1$  powers only and then subtract their sum from  $T$ .

Both bit and power allocation are theoretically unnecessary for the GMD. Since all weights are the same for the SISO channels obtained by the GMD, the power can indeed be equally distributed if also all  $m_l$  are the same. However, it is not immediately clear why the bit allocation is unnecessary, aside from the practical reason that equally strong layers can transmit the equal amount of information. Besides, these statements are usually true only asymptotically (for high SNRs). Therefore, we seek to study how the GMD behaves under bit allocation also experimentally in Section 4.

### 3.2 Power Allocation

Once the number of transmitted bits per symbol is fixed, a further approach to BER minimization is to reassign the initially uniformly distributed transmission power. Assigning more power to layers with small  $\lambda_l$  seems a good strategy to improve the overall BER since small  $\lambda_l$  lead to large values of bit error probability  $p_b^{(l)}$  per MIMO layer  $l$  as implied by the upper bound in Eq. (10) (which is however not always true if both bit and power allocation are performed, cf. Page 793). The task here is

$$p_b(\pi_1, \dots, \pi_L) \xrightarrow{\pi_1 \dots \pi_L} \min \quad \text{s.t.} \quad \sum_{l=1}^L \pi_l^2 = L \quad \text{where} \quad P_s^{(l)} = \frac{\pi_l^2 P_s}{L} . \quad (17)$$

The Lagrange multipliers method is formulated for this task using the following cost function:

$$J(\pi_1 \dots \pi_L, \mu) = \frac{2}{T} \sum_{l=1}^L \left( 1 - 2^{-\frac{m_l}{2}} \right) \quad (18)$$

$$\cdot \operatorname{erfc} \left( \frac{\pi_l \lambda_l}{2\sigma} \sqrt{\frac{3 \cdot P_s}{L(2^{m_l} - 1)}} \right) + \mu \left( \sum_{l=1}^L \pi_l^2 - L \right) \rightarrow \min,$$

where  $\pi_1 > 0, \dots, \pi_L > 0$  are the power allocation parameters with which we modify the initially assigned power  $P_s^{(l)}$  in order to improve  $p_b$  from Eq. (8). With the notations

$$k_l = k_l(m_l, T) := \frac{2}{T} \cdot \left( 1 - 2^{-\frac{m_l}{2}} \right), \quad (19)$$

$$c_l = c_l(m_l, \sigma, P_s, L) := \frac{1}{2\sigma} \sqrt{\frac{3 \cdot P_s}{L(2^{m_l} - 1)}}, \quad l = 1 \dots L, \quad (20)$$

the Lagrange multipliers approach produces the nonlinear system of equations (21) for the minimizer candidates of the cost function (18) :

$$\frac{\partial J(\pi_1 \dots \pi_L, \mu)}{\partial \pi_l} = -\frac{2k_l}{\sqrt{\pi}} \left( c_l \lambda_l e^{-c_l^2 \lambda_l^2 \pi_l^2} \right) + 2\mu \pi_l = 0, \quad \sum_{l=1}^L \pi_l^2 - L = 0, \quad (21)$$

where  $\pi_l > 0, l \in \{1, \dots, L\}$ . It is clear from the first  $L$  equations that  $\mu$  must be positive. Additionally, the second derivative  $\frac{\partial^2 J}{\partial \pi_l \partial \pi_m} = 0$  for  $l \neq m$  and is positive for  $l = m$ . The bordered Hessian is symmetric and has the form

$$\begin{pmatrix} 0 & 2\pi_1 & \dots & 2\pi_L \\ 2\pi_1 & 2\mu + \frac{4k_1 c_1^2 \lambda_1^2}{\sqrt{\pi}} \pi_1 e^{-c_1^2 \lambda_1^2 \pi_1^2} & \dots & 0 \\ 2\pi_2 & 0 & \dots & 0 \\ \vdots & \vdots & \ddots & \vdots \\ 2\pi_L & 0 & \dots & 2\mu + \frac{4k_L c_L^2 \lambda_L^2}{\sqrt{\pi}} \pi_L e^{-c_L^2 \lambda_L^2 \pi_L^2} \end{pmatrix}.$$

It could be shown that the determinants of all relevant  $L-1$  leading principal minors are always negative [1]. For one constraint, this means that a stationary point is a local minimum. Using again the solver for systems of non-linear equations from C-XSC Toolbox, we can compute guaranteed enclosures for all stationary points in the search interval  $(0, L]$  for each  $\pi_l$  from the system in Eq. (21). Working in a verified way has the advantage of taking care of numerical errors. For power allocation, it has an additional benefit of proving that the solution is really unique if only one possibility is suggested. Combined with the analytical conclusions above, this leads to the computer-assisted proof that the candidate obtained by solving (21) is actually the global minimum.

### 3.3 Bit and Power Allocation

The approximate bit and exact power allocation can be performed simultaneously:

$$p_b(\pi_1 \dots \pi_L, m_1, \dots, m_L) \xrightarrow{\pi_1 \dots \pi_L, m_1, \dots, m_L} \min \quad \text{s.t.} \quad \sum_{l=1}^L m_l = T, \quad \sum_{l=1}^L \pi_l^2 = L, \tag{22}$$

where  $P_s^{(l)} = \frac{\pi_l^2 P_s}{L}$ . The cost function combining those from Eq. (14) and (18)

$$J(\pi_1 \dots \pi_L, m_1, \dots, m_L, \mu_1, \mu_2) = \frac{2}{T} \sum_{l=1}^L \left(1 - 2^{-\frac{m_l}{2}}\right) \cdot \operatorname{erfc} \left( \frac{\pi_l \lambda_l}{2\sigma} \sqrt{\frac{3 \cdot P_s}{L(2^{m_l} - 1)}} \right) + \mu_1 \left( \sum_{l=1}^L m_l - T \right) + \mu_2 \left( \sum_{l=1}^L \pi_l^2 - L \right) \tag{23}$$

needs then to be minimized. The corresponding non-linear system for the stationary points is

$$\frac{\partial J}{\partial \pi_l} = -\frac{2k_l}{\sqrt{\pi}} \left( c_l \lambda_l e^{-c_l^2 \lambda_l^2 \pi_l^2} \right) + 2\mu_1 \pi_l = 0 \tag{24}$$

$$\frac{\partial J}{\partial m_l} = \frac{\ln 2}{T} \cdot \left( 2^{-m_l/2} \cdot \operatorname{erfc} (c_l \lambda_l \pi_l) + \frac{2c_l \lambda_l \pi_l 2^{m_l/2}}{(2^{m_l/2} + 1)} \cdot \exp (-c_l^2 \lambda_l^2 \pi_l^2) \right) + \mu_2 = 0$$

$$\frac{\partial J}{\partial \mu_1} = \sum_{l=1}^L m_l - T = 0, \quad \frac{\partial J}{\partial \mu_2} = -T + \sum_{l=1}^L \pi_l^2 = 0 \quad \text{for } l = 1 \dots L$$

having now double the number of equations compared to problems in (14) or (18) individually. In Subsection 4.3, we compare this approach to the approach combining exact power allocation by Eq. (18) and exact bit allocation by brute-force combinatorial approach from points of view of both the BER and computing time for a system with two active layers.

Note that it is possible to solve the problems in Eq. (14) or (18) directly (without having to formulate the respective non-linear systems of equations for the candidates) in the verified way by using global optimization algorithms implemented, for example, within the same C-XSC Toolbox. However, the achieved parameter enclosures are too wide as discussed in [3]. That is why we concentrate on solving the systems of non-linear equations in (15)-(16), (21), (24) using verified methods in this paper, which produces almost point enclosures.

## 4 Numerical Results

In this section, we first take a closer look at the bit allocation for both SVD and GMD based approaches, since it does not seem to be inherently clear that GMD requires the uniform bit distribution in all cases (Subsection 4.2). For this purpose, we consider both an uncorrelated and correlated MIMO system, with 5000 channel realizations each, this benchmark described in Subsection 4.1. After that, we focus on the case of two active layers and compare both approaches in more detail, including power allocation (Subsection 4.3).

### 4.1 The Benchmark System

The practical problem we consider in this paper is a wireless frequency flat MIMO link with  $n_T = n_R = 4$  antennas, the desired constant throughput  $T = 8$  (bit/s)/Hz and the available transmit power  $P_s = 1$ W. In this setup, correlated and uncorrelated data sets with 5000 realizations for  $\lambda_1, \dots, \lambda_4$  each were generated in a non-verified simulation with  $\delta^2 = \frac{1}{2}$ . The correlation coefficients at the transmitter and receiver sides were chosen as  $\rho^{(\text{RX})} = \rho^{(\text{TX})} = 0.2375$  (see [1] for details as well as [6] for an overview on models and [17] for validity areas of the employed Kronecker channel model). If not mentioned otherwise, we provide results at the SNR of  $\frac{E_s}{N_0} = 10$ dB ( $\sigma^2 = 0.05$ ). All simulations in this paper are carried out using Intel i7-4790K @ 4.00GHz (8 cores) CPU under Ubuntu 20.04 LTS and are implemented using C++.

### 4.2 SVD vs GMD: Bit Allocation

In [1], we tested the correlated and uncorrelated MIMO systems described above with their 5000 realizations using verified power allocation and manual bit allocation for the SVD based approach under the restriction  $m_1 \geq m_2 \geq \dots m_L$  with two, three or four active layers. In this subsection, we take a closer look at the bit allocation for both the SVD and GMD based approach, considering two versions.

The first variant (denoted ‘NLI’ for convenience in the following) implements the brute force approach of computing the BER using interval arithmetic for all possible combinations of  $m_l = \log_2 M_l$  (cf. Section 3.1.1). The second variant (denoted ‘OPT’) solves the system of non-linear equations in Eqs. (15)–(16) using the corresponding verified solver from C-XSC Toolbox to obtain enclosures of approximate real values for  $m_l$  (cf. Section 3.1.2). Using methods with result verification, we can, in a guaranteed way, rule out the situation that there exist different, better local minimizers in the considered search interval if the unique solution is obtained.

In Table 1, the results are summarized for four representative examples. First, we consider a randomly chosen uncorrelated data set (№4998, Case 1) and a randomly chosen correlated data set (№101, Case 3) from the available 5000 realizations for each case. For both uncorrelated and correlated MIMO systems, we examine additionally the worst case by taking the smallest values for every of the four  $\lambda_l$  out of the 5000 realizations (Case 2 and 4, respectively). By the formula in Eq. (10), these values provide an upper bound for the achievable BER for all the 5000 realizations considered. Note that this conservative upper bound on the BER of our realizations is not attained by any of the actual realizations since the lower bounds on each of  $\lambda_i$  are not necessarily contained in a single set  $\lambda_1, \dots, \lambda_L$ . All possible values of the BER are below this bound. In Columns 2–6 of the Table, the values of  $m_l$  and the BER for the SVD based approach are given for a predefined number of active layers  $L$  (Column 1) and both variants OPT (the first of the corresponding lines) and NLI (where the integer numbers are given). The structure of Columns 7–11 describing the GMD based approach is the same aside from the additional BER value in parentheses showing, as a comparison, the SVD based BER for the  $m_l$  values optimal for the GMD. The results are computed for the SNR of 10dB.

We reproduce the midpoints of the obtained enclosures for  $m_l$  and the upper bounds of the obtained intervals for the BER; all values are rounded to five digits. The solver in OPT is used with the tolerance of  $10^{-10}$  and the search interval of  $[0.9, 8.1]$  for each of the  $m_l$  along with the  $[-2, 0]$  for the  $\mu$ . The width of the obtained intervals has the maximum order of magnitude of  $10^{-10}$ . Sometimes, OPT could not verify a solution in the chosen search interval (denoted by – in the Table). One reason is that values below one are suggested for weaker layers (agreeing also with the results from non-verified solvers). However, this would correspond to switching the weaker layer off, which we want to explicitly control by choosing the number of active layers  $L$  manually. That is why we do not provide an OPT solution in these cases.

The values computed by OPT always agree with NLI in the sense that positive integers closest to the real values from OPT are also suggested for  $m_l$  by the NLI. This indicates that the system in Eqs. (15)–(16) can be used in combination with verified or non-verified solvers to compute approximate values for  $m_l$  if the NLI approach takes too long for the given number of active layers and the throughput. Obviously, the OPT based BER is somewhat better than the corresponding NLI based one. Verified computations using both NLI and OPT confirm that the GMD based approach is indeed on average at its optimal for equal numbers of bit per symbol  $m_l$ . Using three active layers  $L = 3$  is not a good scenario for GMD for our

benchmark systems since we cannot achieve the throughput of  $T = 8$  with equal  $m_l$  that are positive integers. It is nonetheless interesting that  $m_l = \frac{T}{3}$  is indeed the best choice at a relatively low SNR of 10dB as confirmed by the OPT solution.

In the last example of correlated worst case there were 4 candidates for the system's solution for  $L = 3$  (in italics) if the OPT was used. The expected solution  $m_l = T/L$  is actually not the only one producing the minimum for the BER, there are three more. Since the real solution needs to be rounded to positive integers, those further candidates can be taken as corresponding to 3 possibilities to assign the numbers 3,3,2 to the three  $m_l$ . The order is not important for the GMD based approach since the parameters of the  $p_b^{(l)}$  are otherwise equal. The BER for the GMD is the same for all possibilities and is given in the Table. The best BER for these  $m_l$  with SVD is actually produced by the sequence 3 – 2 – 3 ( $1.9214 \cdot 10^{-1}$ ). It is, however, higher than that for the optimal set 5 – 2 – 1 reproduced in the Table.

Bit allocation does not bring improvement for the GMD in most of the cases from Table 1 at 10dB. However, the best BER under GMD is achieved for 1,1,1,5 (or any other permutation of these numbers) in the uncorrelated and correlated worst case (0.2990 and 0.3633, respectively). As will be shown in the next subsection, there is also one case at 5dB where bit allocation makes sense for the GMD with  $L = 2$  active layers. That is, the bit allocation cannot be ruled out for the GMD and low SNRs.

If bit allocation is performed, the SVD is mostly better than the GMD wrt. the BER at 10dB for the considered examples (if we take into account only positive integer values  $m_l$  relevant in the practice). Without the bit allocation, the GMD can be better on average, especially, in the “normal” cases 1 and 3, where it is so independently of the number of the activated layers. Bit allocation is demonstrated to significantly improve the SVD based BER for both uncorrelated and correlated cases. Without bit allocation, the GMD based approach improves the BER especially in the normal uncorrelated case. In the next subsection, we offer a broader comparison taking into account all 5000 realizations of the uncorrelated and correlated system for two active layers.

As a general observation from this subsection, it could be mentioned that it does not make sense to use all four available layers as also followed from our study of SVD under bit and power allocation in [1]. Employing GMD instead of SVD does not seem to change the situation. It is necessary to perform more experiments to substantiate this claim, which is the subject of our future work.

### 4.3 Detailed Comparison of SVD and GMD for Two Active Layers

In this subsection, we compare in detail how the GMD and SVD based approaches perform for different possibilities in case two layers are switched off in the example system described in Subsection 4.1 ( $L = 2$ ). We consider the same example cases as in the previous subsection at different SNRs. Additionally, we analyze all 5000 realizations of the uncorrelated and correlated channel at different SNRs.

Table 1: Comparison between GMD and SVD wrt. optimal values for  $m_l = \log_2 M_l$  without power allocation at 10dB.

SVD					GMD						
$L$	$m_1$	$m_2$	$m_3$	$m_4$	BER	$m_1$	$m_2$	$m_3$	$m_4$	BER GMD	(BER SVD)
Case 1: uncorrelated data set $\lambda_1 = 4.341226$ , $\lambda_2 = 2.178729$ , $\lambda_3 = 1.070086$ , $\lambda_4 = 0.474591$ , $\vartheta \approx 0.11$											
2	4.9113	3.0887			$7.1359 \cdot 10^{-4}$	4	4			$7.8821 \cdot 10^{-4}$	(55.061 · 10 <sup>-4</sup> )
	5	3			$7.5104 \cdot 10^{-4}$	4	4			$7.8821 \cdot 10^{-4}$	(55.061 · 10 <sup>-4</sup> )
3	4.3079	2.5510	1.1410		$7.2862 \cdot 10^{-4}$	$\frac{8}{3}$	$\frac{8}{3}$	$\frac{8}{3}$		$14.032 \cdot 10^{-4}$	(220.67 · 10 <sup>-4</sup> )
	4	3	1		$16.148 \cdot 10^{-4}$	3	3	2		$31.536 \cdot 10^{-4}$	(78.309 · 10 <sup>-4</sup> )
4	–	–	–	–	–	2	2	2	2	$96.220 \cdot 10^{-4}$	(680.30 · 10 <sup>-4</sup> )
	4	2	1	1	$149.04 \cdot 10^{-4}$	2	2	2	2	$96.220 \cdot 10^{-4}$	(680.30 · 10 <sup>-4</sup> )
Case 2: uncorrelated, worst case $\lambda_1 = 2.420786$ , $\lambda_2 = 0.917965$ , $\lambda_3 = 0.302213$ , $\lambda_4 = 0.004891$ , $\vartheta \approx 0.002$											
2	5.2343	2.7657			$4.6972 \cdot 10^{-2}$	4	4			$5.1015 \cdot 10^{-2}$	(7.0148 · 10 <sup>-2</sup> )
	5	3			$4.7907 \cdot 10^{-2}$	4	4			$5.1015 \cdot 10^{-2}$	(7.0148 · 10 <sup>-2</sup> )
3	–	–	–	–	–	$\frac{8}{3}$	$\frac{8}{3}$	$\frac{8}{3}$		$10.458 \cdot 10^{-2}$	(13.418 · 10 <sup>-2</sup> )
	5	2	1		$7.1372 \cdot 10^{-2}$	3	3	2		$10.916 \cdot 10^{-2}$	(11.730 · 10 <sup>-2</sup> )
4	–	–	–	–	–	2	2	2	2	$35.252 \cdot 10^{-2}$	(22.167 · 10 <sup>-2</sup> )
	4	2	1	1	$13.694 \cdot 10^{-2}$	2	2	2	2	$35.252 \cdot 10^{-2}$	(22.167 · 10 <sup>-2</sup> )
Case 3: correlated data set $\lambda_1 = 3.9493$ , $\lambda_2 = 1.6891$ , $\lambda_3 = 0.9149$ , $\lambda_4 = 0.3578$ , $\vartheta \approx 0.091$											
2	5.1129	2.8871			$3.2611 \cdot 10^{-3}$	4	4			$3.6752 \cdot 10^{-3}$	(17.115 · 10 <sup>-3</sup> )
	5	3			$3.4050 \cdot 10^{-3}$	4	4			$3.6752 \cdot 10^{-3}$	(17.115 · 10 <sup>-3</sup> )
3	4.4896	2.3487	1.1616		$3.3103 \cdot 10^{-3}$	$\frac{8}{3}$	$\frac{8}{3}$	$\frac{8}{3}$		$5.6410 \cdot 10^{-3}$	(34.968 · 10 <sup>-3</sup> )
	5	2	1		$5.6579 \cdot 10^{-3}$	3	3	2		$9.4616 \cdot 10^{-3}$	(18.886 · 10 <sup>-3</sup> )
4	–	–	–	–	–	2	2	2	2	$27.299 \cdot 10^{-3}$	(90.895 · 10 <sup>-3</sup> )
	4	2	1	1	$26.776 \cdot 10^{-3}$	2	2	2	2	$27.299 \cdot 10^{-3}$	(90.895 · 10 <sup>-3</sup> )
Case 4: correlated, worst case $\lambda_1 = 1.3791$ , $\lambda_2 = 0.5526$ , $\lambda_3 = 0.1609$ , $\lambda_4 = 0.0013$ , $\vartheta \approx 0.0009$											
2	5.6754	2.3246			$1.3631 \cdot 10^{-1}$	4	4			$1.4350 \cdot 10^{-1}$	(1.4033 · 10 <sup>-1</sup> )
	6	2			$1.3667 \cdot 10^{-1}$	4	4			$1.4350 \cdot 10^{-1}$	(1.4033 · 10 <sup>-1</sup> )
3	–	–	–	–	–	$\frac{8}{3}$	$\frac{8}{3}$	$\frac{8}{3}$		$2.2482 \cdot 10^{-1}$	(2.0133 · 10 <sup>-1</sup> )
	5	2	1		$1.7307 \cdot 10^{-1}$	3	3	2		$2.2418 \cdot 10^{-1}$	(1.9441 · 10 <sup>-1</sup> )
4	–	–	–	–	–	2	2	2	2	$4.2949 \cdot 10^{-1}$	(2.7613 · 10 <sup>-1</sup> )
	4	2	1	1	$2.3086 \cdot 10^{-1}$	2	2	2	2	$4.2949 \cdot 10^{-1}$	(2.7613 · 10 <sup>-1</sup> )



From Figure 3, it can be seen that the GMD approach is better than the one based on the SVD if resources are allocated uniformly ( $P_s^{(l)} = \frac{1}{2}W$ ,  $m_l = 4$ ,  $l = 1, 2$ ). The Figure shows the comparison for the example systems with 5000 realizations each (uncorrelated on the left, correlated on the right) at 10dB and 15dB. For clarity of the representation, only every 100th result is shown. For frequency plots on  $\lambda_l$ , see [1].

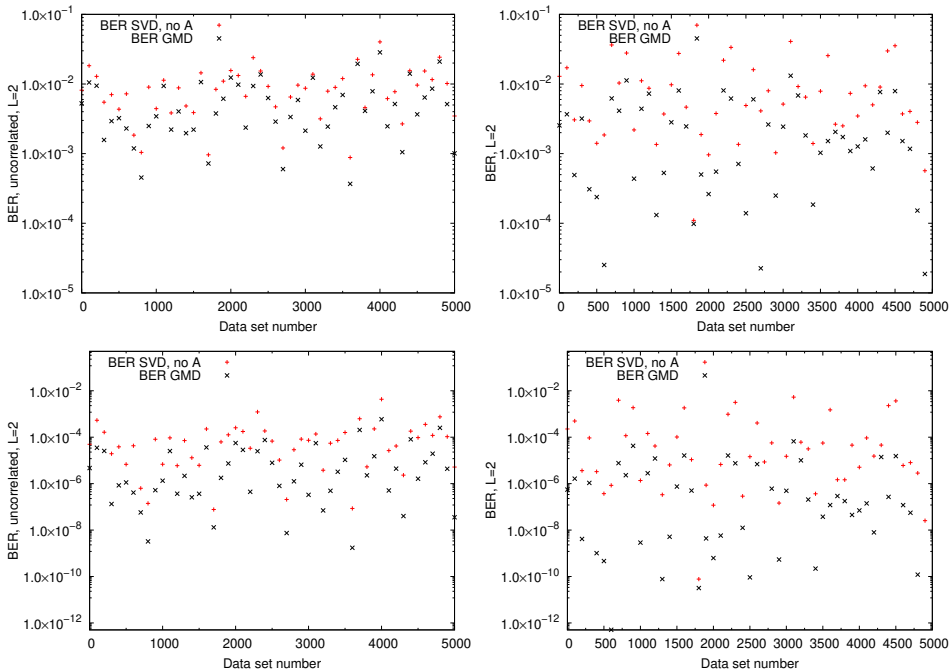


Figure 3: BER for SVD and GMD without any resource allocation for 5000 realizations (with every 100th result shown) of an uncorrelated (left) and correlated (right) MIMO link at 10dB (above) and 15dB (below).

In Figure 4, the comparison between the BER for the GMD based approach with uniformly allocated resources and SVD without power allocation but with bit allocation by OPT is shown, again for 5000 realizations of the uncorrelated and correlated MIMO channels at 10dB and 15dB. The SVD based approach with bit allocation is always better than the GMD one in this case. The unique optimum for  $m_l$  cannot always be verified. While optimal solutions can be verified for all 5000 channel realizations in the non-correlated case, 10 cases are not solved for the correlated channel. At 15dB, the corresponding numbers for unsolved cases are 2435 and 3661, respectively. In this subsection, the optimum was considered as not verified if there was no solution to the system in Eqs. (15)–(16) with  $L = 2$  in the considered search interval or if there were multiple solutions.

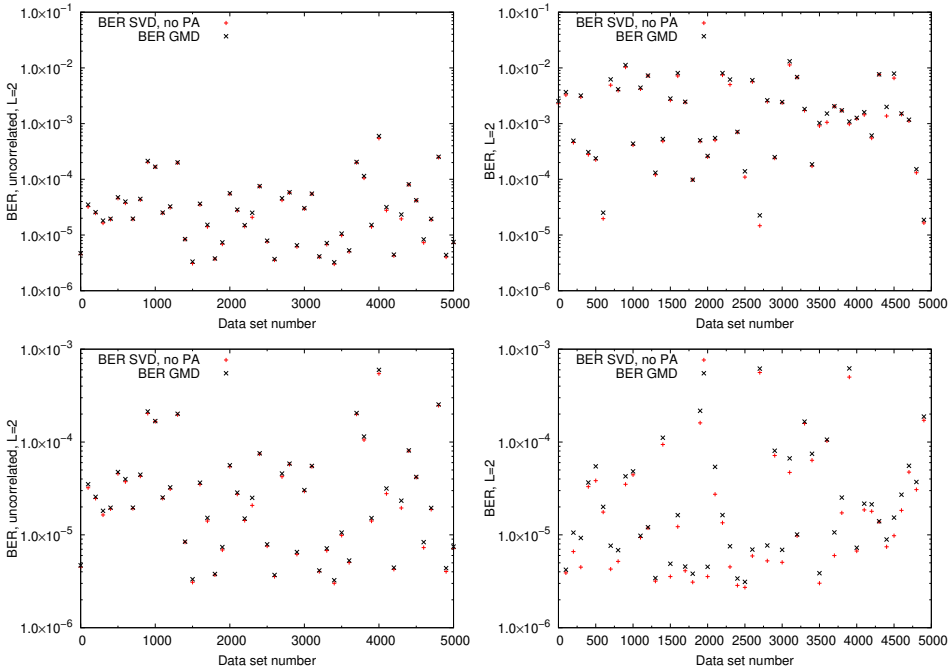


Figure 4: BER for SVD with bit allocation and GMD for 5000 realizations (with every 100th result shown) of an uncorrelated (left) and correlated (right) MIMO link at 10dB (above) and 15dB (below).

Next, we consider how the examples from Table 1 behave if both bit and power allocation (BPA) are performed for the SVD separated channels using the NLI and OPT approaches at different SNRs. Here, NLI means that the system in Eqs. (15)–(16) is solved by C-XSC for each admissible combination of  $m_l$  computed by a brute force approach to identify the combination leading to the smallest BER. For OPT, we solve the system in Eq. (24) using C-XSC. In case of the GMD, we perform only bit allocation as a comparison and for the sake of completeness. There is only one case where non-uniform bit allocation is better for the GMD. Therefore, we provide the numbers for  $m_l$  in this case only. The results are given in Table 2. For BPA with OPT, the numbers given for  $m_l$  are the closest integers. We see that there is no difference in  $m_l$  if we do bit and parameter allocation separately by verified non-linear equations solver and optimization (NLI) or together using the system in Eq. (24) by a non-linear solver (OPT) as long as  $T$  is fixed. There is, as expected, a difference in the BER, although not very large. From Table 2, it is evident that not only power but also bit allocation depend on both  $\sigma$  and  $\lambda_l$  and cannot be precomputed. Although, at least for smaller  $\sigma$ , the BER of GMD is sometimes better than that of SVD after bit allocation, power allocation makes the BER for

the SVD separated channels the best in all of the considered cases.

Note that the assumption that power allocation assigns more power to weaker layers is not always correct as demonstrated for  $L = 2$ . For example in Case 3, the power  $\pi^2 \cdot P_s^{(1)}$  assigned to the first (and strongest) layer with  $\lambda_1 = 3.9493$  is approximately 0.54361 W ( $\pi_1 \approx 1.0427$ ), whereas the second layer with  $\lambda_2 = 1.6891$  is assigned 0.45639 W ( $\pi_2 \approx 0.95539$ ) to achieve the minimal BER of  $3.2192 \cdot 10^{-3}$  at  $m_1 \approx 5.2254$ ,  $m_2 \approx 2.8871$  and the SNR of 10dB given in Table 2 if OPT is used. This is true for all 5000 data sets and is similar for the uncorrelated channel (0.53164 W for the first layer, 0.46836 W for the second in Case 1): the stronger layer is always assigned more power for two active layers at 10dB.

Table 2: Comparison between the GMD and SVD based BER under bit and power allocation for two active layers and the examples from Table 1.

	dB	BER SVD			BER GMD
		BA	BPA (NLI)	BPA (OPT)	BA (4-4)
Case 1	5	$3.0196 \cdot 10^{-2}(5-3)$	$2.9767 \cdot 10^{-2}(5-3)$	$2.9767 \cdot 10^{-2}(5-3)$	$3.1398 \cdot 10^{-2}$
	10	$7.5104 \cdot 10^{-4}(5-3)$	$7.0689 \cdot 10^{-4}(5-3)$	$7.0686 \cdot 10^{-4}(5-3)$	$7.8821 \cdot 10^{-4}$
	15	$1.8489 \cdot 10^{-8}(5-3)$	$1.2815 \cdot 10^{-8}(5-3)$	–	$1.6971 \cdot 10^{-8}$
Case 2	5	$1.4185 \cdot 10^{-1}(6-2)$	$1.3980 \cdot 10^{-1}(6-2)$	$1.3933 \cdot 10^{-1}(6-2)$	$1.5070 \cdot 10^{-1}$
	10	$4.7907 \cdot 10^{-2}(5-3)$	$4.7895 \cdot 10^{-2}(5-3)$	$4.6371 \cdot 10^{-2}(5-3)$	$5.1015 \cdot 10^{-2}$
	15	$3.2918 \cdot 10^{-3}(5-3)$	$2.8633 \cdot 10^{-3}(5-3)$	$2.5074 \cdot 10^{-3}(5-3)$	$3.0105 \cdot 10^{-3}$
Case 3	5	$5.1756 \cdot 10^{-2}(5-3)$	$5.1672 \cdot 10^{-2}(5-3)$	$5.1168 \cdot 10^{-2}(5-3)$	$5.4896 \cdot 10^{-2}$
	10	$3.4050 \cdot 10^{-3}(5-3)$	$3.3502 \cdot 10^{-3}(5-3)$	$3.2192 \cdot 10^{-3}(5-3)$	$3.6753 \cdot 10^{-3}$
	15	$1.9868 \cdot 10^{-6}(5-3)$	$1.3623 \cdot 10^{-6}(5-3)$	–	$1.6392 \cdot 10^{-6}$
Case 4	5	$1.9676 \cdot 10^{-1}(7-1)$	$1.9618 \cdot 10^{-1}(7-1)$	–	$2.0156 \cdot 10^{-1}(7-1)$ $2.3381 \cdot 10^{-1}$
	10	$1.3667 \cdot 10^{-1}(6-2)$	$1.3441 \cdot 10^{-1}(6-2)$	$1.3440 \cdot 10^{-1}(6-2)$	$1.4350 \cdot 10^{-1}$
	15	$4.2405 \cdot 10^{-2}(5-3)$	$4.2404 \cdot 10^{-2}(5-3)$	$4.1433 \cdot 10^{-2}(5-3)$	$4.5213 \cdot 10^{-2}$

The fact that SVD is better than the GMD if both bit and power allocation is performed using OPT at all SNRs, observed for the four examples in Table 2, is confirmed by the simulation considering all 5000 realizations of the uncorrelated and correlated channel (cf. Figure 5). At 10dB, the minimum could not be verified for 11 data sets in the correlated case using OPT. SVD with BPA is better than GMD in all the remaining cases. At 15dB, the result could not be verified for 3667 (correlated) and 2441 (uncorrelated) data sets using OPT. For the remaining data sets, SVD is better. Note that, although the OPT approach is quite helpful if only bit allocation is performed since it identifies the optimal  $m_l$  constellations reliably, it is purely theoretical if both bit and power allocation are combined as in

Eq. (24). The optimal power parameters  $\pi_l$  obtained for the real values of  $m_l$  do not necessarily retain their optimality for the corresponding positive integer  $m_l$ .

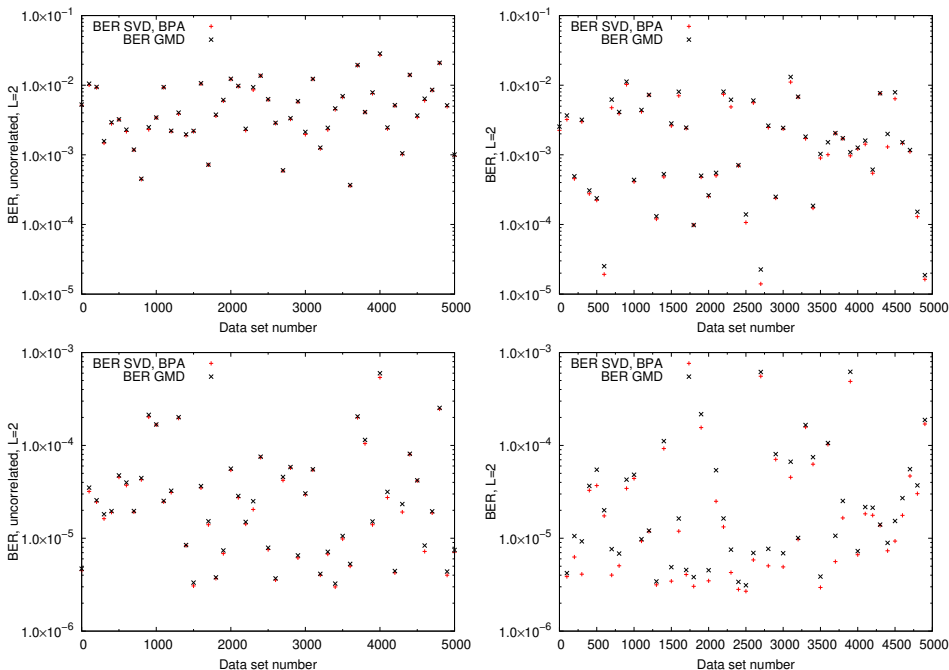


Figure 5: BER for SVD with bit and power allocation and GMD without resource allocation for 5000 realizations (with every 100th result shown) of an uncorrelated (left) and correlated (right) MIMO link at 10dB (above) and 15dB (below).

Using NLI for both bit and power allocation is more relevant in practice. On the one hand, more information can be gained with respect to GMD/SVD comparison since a verified proof of uniqueness is possible for almost all data sets<sup>4</sup>. The reason for this is that only two equations need to be solved for each  $m_1 - m_2$  combination in the verified way. On the other hand, the NLI approach uses only positive integer constellations of  $m_l$ , leading to realistic values of  $\pi_l$  and the BER.

If BPA for the SVD case is performed via NLI, the SVD based channel separation is not always better as demonstrated in Figure 6, on the left. There, the normalized ratio is shown between the number of cases in which the BER under SVD is better for 5000 realizations of uncorrelated/correlated MIMO systems and the overall number of successful cases. Note that the resources are allocated uniformly in the GMD case. At lower SNRs, SVD is better, especially in the correlated case. At

<sup>4</sup>For example, a verified result cannot be produced for overall 79 combinations in the correlated case using NLI at 15dB, which also includes combinations possibly not leading to the minimal BER

higher SNRs, GMD is better, especially in the uncorrelated case. On the right of Figure 6, the best and worst computed values of the BER are shown at each SNR for correlated and uncorrelated MIMO system under SVD and GMD for 5000 realizations each. We observe that the GMD is mostly better in terms of the upper and lower bounds. That is, out of 5000 realizations, the smallest best case bound (lower) and the smallest worst case bound (upper) are provided by GMD (starting at 12.5dB, at the latest). This does not mean that this is so on average (cf. the Figure on the left). Additionally, it can be seen that the correlated MIMO system has a much broader intervals between the best and the worst achievable BER within the same channel.

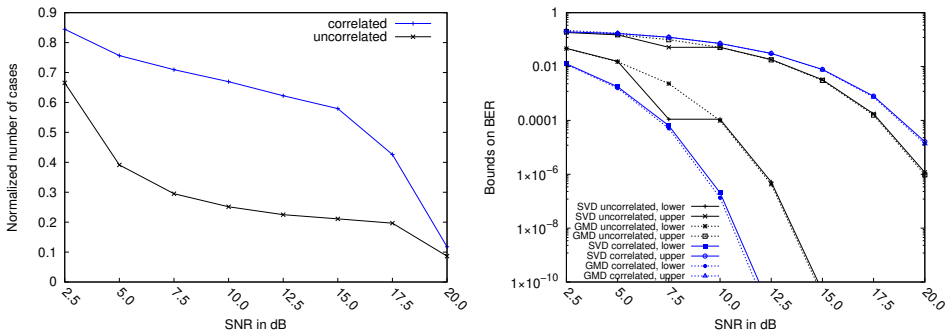


Figure 6: On the left, the normalized number of cases of better BER under SVD and NLI. On the right, lower and upper BER bounds under SVD (solid) and GMD (dashed). In both figures, 5000 realizations of the uncorrelated (black) and correlated (blue) MIMO systems are considered.

To give an idea about the computing times, we provide the user CPU time supplied by the Ubuntu function `time` for the slowest simulation variant (5000 realizations, BPA). While the simulations are run as a matter of seconds for variants with only bit or only power allocation (or, of course, without any resource allocation), the user time is 80 minutes for OPT in the correlated, 52 minutes in the uncorrelated case and on average 17 seconds both for correlated and uncorrelated case using NLI if BPA is performed at 10dB. This time includes output operations (creating a text file with data for Figures 5 or 6, respectively). Note that NLI is much faster because there are only seven possibilities to check for two active layers.

## 5 Conclusions

In this paper, we studied bit and power allocation for the SVD based channel separation from the verified point of view. Additionally, we compared the results to the GMD-based approach, not only from the theoretical side but also using 5000 realizations of an uncorrelated and correlated MIMO channel. Although the GMD

based approach is considered to require no resource allocation, at least asymptotically for high SNR, it is not always so at lower SNRs, where bit allocation might be profitable in isolated cases. Experimentally, we demonstrated that the GMD is definitely an alternative if no optimization of resource allocation can be carried out. Besides, it is competitive even if there is enough capacity to perform bit and power allocation for the SVD separated channel, at least, for higher SNRs, especially under good scattering conditions. However, the SVD outperforms the GMD wrt. to the quality criterion of the BER on average in bad scattering conditions and lower SNRs. As concerns the SVD based channel separation, we observe that using only bit allocation improves the BER significantly for both uncorrelated and correlated MIMO systems. The BER can be improved even further by subsequent power allocation, the adjustment for the better more visible in the uncorrelated than in the correlated case.

Some of the results suggest that employing GMD instead of SVD does not change the fact that the weakest layer should be switched off, at least, at lower SNRs. More experiments are necessary to substantiate this suggestion, which is the topic for our future work. Additionally, it is not clear beforehand for given singular values and an SNR whether the BER would be better if SVD or GMD is employed. A comprehensible criterion depending on these parameters would help to optimize MIMO systems further wrt. their BER. To study if it is possible to devise such a criterion is a further subject for our future work.

## References

- [1] Auer, E. and Ahrens, A. Guaranteed minimization of the bit error ratio for correlated MIMO systems. In *Proceedings of the 9th International Workshop on Reliable Engineering Computing*, pages 457–470, 2021. URL: [http://ww2new.unime.it/REC2021/proceedings/REC2021\\_Proceedings.pdf](http://ww2new.unime.it/REC2021/proceedings/REC2021_Proceedings.pdf).
- [2] Auer, E. and Ahrens, A. Guaranteed minimization of the bit error ratio for MIMO systems: A mathematical viewpoint. *ASCE-ASME Journal of Risk and Uncertainty in Engineering Systems Part B: Mechanical Engineering*, 7(2), 2021. DOI: [10.1115/1.4050161](https://doi.org/10.1115/1.4050161).
- [3] Auer, E., Benavente-Peces, C., and Ahrens, A. Solving the power allocation problem using methods with result verification. *International Journal of Reliability and Safety*, 12(1/2):86–102, 2018. DOI: [10.1504/IJRS.2018.092506](https://doi.org/10.1504/IJRS.2018.092506).
- [4] Chiani, M., Win, M. Z., and Zanella, A. On the capacity of spatially correlated MIMO Rayleigh-fading channels. *IEEE Transactions on Information Theory*, 49:2363–2371, 2003. DOI: [10.1109/TIT.2003.817437](https://doi.org/10.1109/TIT.2003.817437).
- [5] de Figueiredo, L. H. and Stolfi, J. Affine arithmetic: Concepts and applications. *Numerical Algorithms*, 34(1–4):147–158, 2004. DOI: [10.1023/B:NUMA.0000049462.70970.b6](https://doi.org/10.1023/B:NUMA.0000049462.70970.b6).

- [6] Ertel, R. B., Cardieri, P., Sowerby, K. W., Rappaport, T. S., and Reed, J. H. Overview of spatial channel models for antenna array communication systems. *IEEE Personal Communications*, 5(1):10–22, 1998. DOI: [10.1109/98.656151](https://doi.org/10.1109/98.656151).
- [7] Foschini, G. Layered space-time architecture for wireless communication in a fading environment when using multi-element antennas. *Bell Labs Technical Journal*, 1(2):41–59, 1996. DOI: [10.1002/bltj.2015](https://doi.org/10.1002/bltj.2015).
- [8] Hofschuster, W., Krämer, W., and Neher, M. C-XSC and closely related software packages. In Cuyt, A. M., Krämer, W., Luther, W., and Markstein, P. W., editors, *Numerical Validation in Current Hardware Architectures*, Volume 5492 of *Lecture Notes in Computer Science*, pages 68–102, 2008. DOI: [10.1007/978-3-642-01591-5\\_5](https://doi.org/10.1007/978-3-642-01591-5_5).
- [9] Jiang, Y., Hager, W. W., and Li, J. The generalized triangular decomposition. *Mathematics of Computation*, 77(262):1037–1056, 2008. DOI: [10.1090/S0025-5718-07-02014-5](https://doi.org/10.1090/S0025-5718-07-02014-5).
- [10] Jiang, Y., Li, J., and Hager, W. W. MIMO transceiver design using geometric mean decomposition. In *Proceedings of the 2004 IEEE Information Theory Workshop*, pages 193–197, San Antonio, TX, USA, 2004. IEEE. DOI: [10.1109/ITW.2004.1405298](https://doi.org/10.1109/ITW.2004.1405298).
- [11] Kuo, P.-H. and Ting, P. Probabilistic behavior analysis of MIMO fading channels under geometric mean decomposition. *Journal of Electrical and Computer Engineering*, pages 1–8, 2012. DOI: [10.1155/2012/340809](https://doi.org/10.1155/2012/340809).
- [12] Lee, J. and Leyffer, S. *Mixed Integer Nonlinear Programming*. Springer Publishing Company, Incorporated, 2011. DOI: [10.1007/978-1-4614-1927-3](https://doi.org/10.1007/978-1-4614-1927-3).
- [13] Lerch, M., Tischler, G., von Gudenberg, J. W., Hofschuster, W., and Krämer, W. filib++, a fast interval library supporting containment computations. *ACM Transactions on Mathematical Software*, 32(2):299–324, 2006. DOI: [10.1145/1141885.1141893](https://doi.org/10.1145/1141885.1141893).
- [14] Lohner, R. On the ubiquity of the wrapping effect in the computation of error bounds. In Kulisch, U., Lohner, R., and Facius, A., editors, *Perspectives on Enclosure Methods*, pages 201–218. Springer-Verlag, 2001. DOI: [10.1007/978-3-7091-6282-8\\_12](https://doi.org/10.1007/978-3-7091-6282-8_12).
- [15] Moore, R. E., Kearfott, R. B., and Cloud, M. J. *Introduction to Interval Analysis*. Society for Industrial and Applied Mathematics, Philadelphia, 2009. DOI: [10.1137/1.9780898717716](https://doi.org/10.1137/1.9780898717716).
- [16] Nedialkov, N. S. *Implementing a Rigorous ODE Solver Through Literate Programming*. In Rauh, A. and Auer, E., editors, *Modeling, Design, and Simulation of Systems with Uncertainties*, Volume 3 of *Mathematical Engineering*,

- pages 3–19. Springer, Heidelberg, 2011. DOI: [10.1007/978-3-642-15956-5\\_1](https://doi.org/10.1007/978-3-642-15956-5_1).
- [17] Oestges, C. Validity of the Kronocker Model for MIMO Correlated Channels. In *Vehicular Technology Conference*, Volume 6, pages 2818–2822, Melbourne, 2006. DOI: [10.1109/VETECS.2006.1683382](https://doi.org/10.1109/VETECS.2006.1683382).
- [18] Raleigh, G. G. and Cioffi, J. M. Spatio-temporal coding for wireless communication. *IEEE Transactions on Communications*, 46(3):357–366, 1998. DOI: [10.1109/26.662641](https://doi.org/10.1109/26.662641).
- [19] Shinde, K. *Interval uncertainty method to treat inconsistent measurements in inverse problems*. PhD thesis, Université de Technologie de Compiègne, 2021. URL: <https://theses.hal.science/tel-03680994>.
- [20] Sklar, B. Rayleigh fading channels in mobile digital communication systems. I. Characterization. *IEEE Communications Magazine*, 35(7):90–100, 1997. DOI: [10.1109/35.601747](https://doi.org/10.1109/35.601747).
- [21] Telatar, E. Capacity of multi-antenna Gaussian channels. *European Transactions On Telecommunications*, 10:585–595, 1999. DOI: [10.1002/ett.4460100604](https://doi.org/10.1002/ett.4460100604).
- [22] Tse, D. and Viswanath, P. *The Wireless Channel*. In *Fundamentals of Wireless Communication*, chapter 2. Cambridge University Press, 2005. DOI: [10.1017/CB09780511807213](https://doi.org/10.1017/CB09780511807213).
- [23] Weikert, O. and Zölzer, U. Efficient MIMO channel estimation with optimal training sequences. In *Proceedings of 1st Workshop on Commercial MIMO Components and Systems*, Duisburg, Germany, 2007.
- [24] Zaiser, S., Buchholz, M., and Dietmayer, K. Interval system identification for MIMO ARX models of minimal order. In *53rd IEEE Conference on Decision and Control*, pages 1774–1779, 2014. DOI: [10.1109/CDC.2014.7039655](https://doi.org/10.1109/CDC.2014.7039655).